http://www.geojournals.cn/dzxbcn/ch/index.aspx

Geochemical Tracing of Ore-forming Material Sources of Carlin-type Gold Deposits in the Yunnan-Guizhou-Guangxi Triangle Area —A Case Study of the Application of the Combined Silicon Isotopes Geochemistry and Siliceous Cathodoluminescence Analysis

LIU Xianfan[1], NI Shijun[2], LU Qiuxia[2], JIN Jingfu[2] and ZHU Laimin[1]

1. *Open Lab of Ore Deposits Geochemistry, Institute of Geochemistry, Chinese Academy of Sciences, Guiyang 550002*

2. *Chengdu Institute of Technology, Chengdu 610059*

Abstract This paper deals with characteristics of silicon isotope compositions and siliceous cathodoluminescence of host rocks, ores and hydrothermal silicified quartz of the Carlin-type ore deposits in the Yunnan-Guizhou-Guangxi triangle area. The study shows that primary silicified quartz is nonluminescent but quartz in host rocks and secondary silicified quartz are luminescent by the action of cathode rays. Correspondingly, silicon isotope compositions of host rocks, ores and hydrothermal quartz veins are clearly distinguished. In strata from the Middle Triassic to the "Dachang" host bed, $\delta^{30}Si$ of the host rocks ranges from 0.0 ‰–0.3 ‰, while that of primary ore-forming silicified fluids from –0.1 ‰ to –0.4 ‰; in the Upper Permian and Lower Carboniferous strata and Indosinian diabase host beds, $\delta^{30}Si$ of the host rocks is from –0.1 ‰ to –0.2 ‰ and that of the primary silicified quartz veins from 0.3 ‰–0.5 ‰. This pattern demonstrates the following geochemical mineralization process: primary ore-forming siliceous fluids migrated upwards quickly along the main passages of deep-seated faults from mantle to crust and entered secondary faults where gold deposits were eventually formed as a result of permeation and replacement of the siliceous ore-forming fluids into different ore-bearing strata. This gives important evidence for the fact that ore-forming fluids of this type of gold deposits were mainly derived from upper mantle differentiation and shows good prospects for deep gold deposits and geochemical background for large and superlarge gold deposits.

Key words: silicon isotope, siliceous cathodoluminescence, tracing of ore-forming material source, Carlin-type gold deposit, Yunnan-Guizhou-Guangxi triangle area

1 Geological Setting of the Ore District and Geology of the Ore Deposits

Belonging to the Dian (Yunnan)-Qian (Guizhou)-Gui (Guangxi) rift valley, the Yunnan-Guizhou-Guangxi triangle area is situated at the junction of the Yangtze block and the Youjiang orogenic belt of the South China Caledonian fold system (Xia et al., 1992) (Fig.1). This area is bounded by the NE-striking Mile-Shizong fault, NW-striking Shuicheng-Ziyun-Bama fault belt and the Wenshan-Guangnan-Funing arc fault belt in the south, which surrounds the Yuebei old land and projects northwards. Within the rift there is a domal structure composed of a set of secondary faults and folded belts. Gold orebodies were formed right in those secondary faults or on the limbs of the domal structure. In these structural belts, early-stage faults were intensely activated during the Indosinian-Yanshanian Period to eventually form giant crust-penetrating faults. Evidence for this geological event can be seen in the following.

(1) Sporadic dyke-like Yanshanian subalkali ultrabasic intrusive rocks and quartz porphyry and granite-porphyry are found in southwestern Guizhou and northwestern Guangxi (Yang et al., 1994). (2) The latest geophysical data (Wang et al., 1995) revealed that ultrabasic-basic-acid magmatic rocks are extensively buried in this area, corresponding to mantle uplift (Fig. 2). (3) Different measurements and analyses have confirmed that gold deposits of this area were generally formed during the period from the late Yanshanian to the early Himalayan (Hu et al., 1995). The

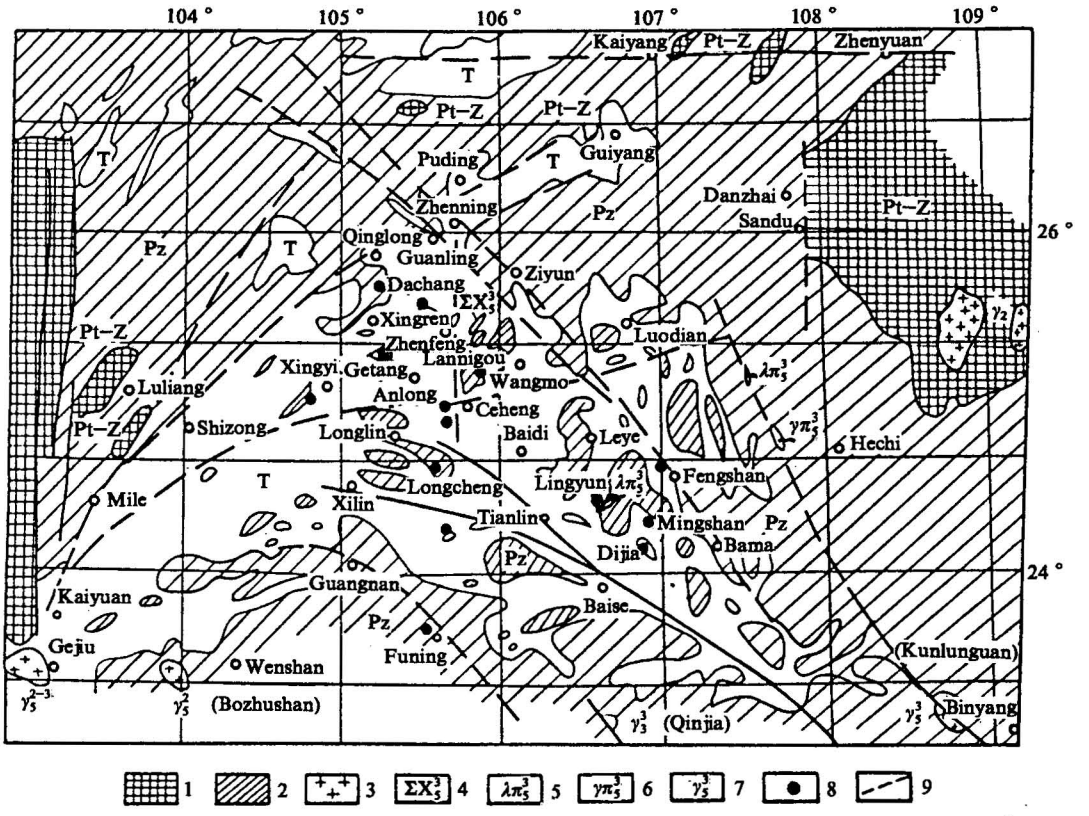

Fig. 1 A sketch map showing regional geology and ore deposits in the Yunnan-Guizhou-Guangxi area (after Yang et al., 1992).

1. Proterozoic-Sinian (Pt-Z); 2. Palaeozoic (Pz); 3. granite intrusion; 4. subalkaline ultrabasic intrusive rocks; 5. quartz porphyry; 6. granitic porphyry; 7. symbol of granite intrusion; 8. gold ore zone (deposit); 9. deep-seated fault.

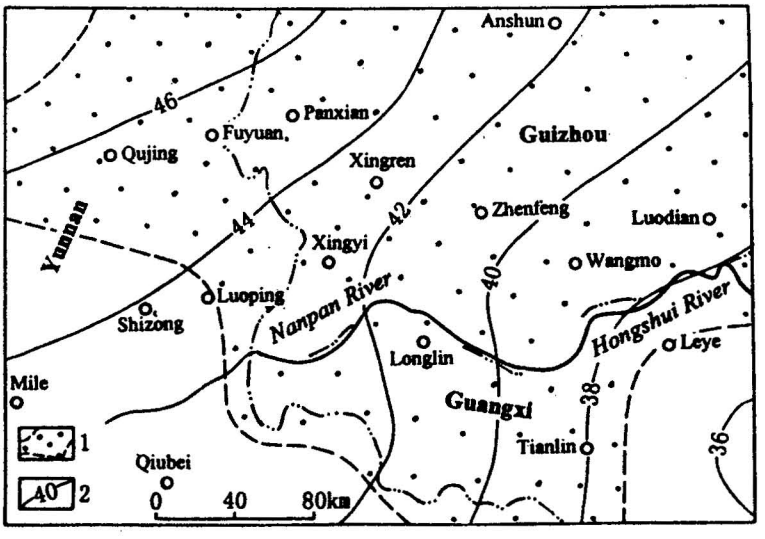

Fig. 2. Moho and density contour map of the upper mantle in the Yunnan-Guizhou-Guangxi area (after Wang et al., 1995).

1. Dense upper mantle; 2. Moho contour.

above facts show that the gold deposits in this area might have a common genesis and that fault structures controlling rifts and gold distribution are characterized by crust-mantle penetration. These faults serve as a favourable passage for deep ore-forming fluids to flow up into the crust to mix with and replaced by shallower fluids, so that gold deposits could form in the deep crust.

The gold ore is hosted in all strata from the Cambrian to the Middle Triassic in this area. The ore deposits were formed in multiple mineralization epochs and multiple ore-bearing horizons, and moreover, a gold-bearing horizon in some areas might not be a host horizon in other areas. The major host rocks include fine clastic rocks, e.g. tuffaceous clastic rocks, and impure carbonate rocks with occasional altered diabase and basalt. This shows that the ore occurrence is primarily related to lithology rather than stratigraphy. However, even ore-bearing lithology does not have specialization for the ore formation, which is also controlled by fault structures and alterations. Lithology is only of significance in respect to ore-bearing space than source beds, indicating that the gold ore here is not typically stratabound and the mineralization has no particular source beds (Ni et al., 1997).

Although different deposits exhibit diversified geological features, they may have many characters in common, i.e. the near-ore hydrothermal alterations basically include silicification, pyritization, arsenopyritization, clayization and carbonatization, and the first two are most closely associated with mineralization. By looking into the relationship between silicification and gold mineralization, this paper discusses possible ore-forming fluids of gold ore by tracing ore-forming siliceous substances. Based on field observation and mineragraphic study, the authors consider that there are two types of silicification: primary and secondary, which correspond to primary and supergene gold mineralizations respectively. Since the latter is a reworked product of the former, one of the important approaches to finding out the primary source of gold mineralization is to correctly distinguish primary silicification from the secondary one so as to trace siliceous source of the primary silicification. An effective method in this aspect should be silicon-isotope geochemistry in combination with siliceous cathodoluminescence analysis.

2 Selection of Samples and Construction of Composite Ore-bearing Section

The samples were selected from representative host rocks, ores and hydrothermal minerals (veins), which are closely related to siliceous materials and quartz, in typical ore-bearing horizons of some important deposits in this area. A sampling composite section of ore-bearing horizons is described from top to bottom (from younger to older) as follows.

(1) Yanshanian quartz porphyry (intruding into the Triassic; Bama of Guangxi,).

(2) Ore: quartz-texture breccia, highly altered cataclasite (in the Triassic; Lannigou and Mingshan).

(3) T_2by and T_2b (Bianyang and Baipeng Formations): Calcareous quartz siltstone and silty mudstone (Lannigou and Mingshan).

(4) Ore and mineralized rocks: silicified breccia (in the Upper Permian and the "Dachang bed"; Getang and Qinglong).

(5) P_2d (Dalong Formation): sponge-spicule siliceous rock (Getang).

(6) $P_2\beta$ (basalt) and P_1d (Dachang bed): weakly altered basaltic breccia (Qinglong).

(7) P_2 and P_1d (Dachang bed): pyrite-bearing crystal tuff (Longhuo).

(8) Ore, mineralized rocks and quartz veins: highly altered diabase, highly silicified breccia, and late-mineralization epoch, post-mineralization and supergene quartz veins (in the Lower Carboniferous and diabase; Longhuo and Shijia).

(9) Indosinian diabase: weakly altered diabase (Shijia).

(10) C_1y (bottom of the Yanguan Formation): weakly altered vitric tuff (Longhuo).

3 Siliceous Cathodoluminescence Analysis

Mineral luminescence may be caused by various factors, which should be analyzed in consideration of concrete cases (Song, 1993). Evidently, characteristics of quartz cathodoluminescence provide significant information in regard to its geological attitude, formation temperature, type and content of activating agents

Table 1 Cathodoluminescence characteristics of different types of siliceous substances and quartz in the gold deposits of the study area

Relation with mineralization	Occurrence mode	Characteristics under microscope	Luminescence characteristics	Typical photo
Host rocks	Sponge-spicule siliceous rock	Circular texture, filled with cryptocrystalline siliceous substance	Light brownish red silica outside and light brown silica inside	III-11 III-12
	Calcareous quartz silty rock	Silty texture, calcareous and argillaceous cementation, subhedral-anhedral clastic quartz, no wavy extinction	Light purple-purple quartz with light brown rim of secondary growth	III-1 III-2 III-13 III-14
	Tuffaceous pyroclastic rock	Tuffy-silty texture, tuffaceous and argillaceous cementation, subhedral-anhedral clastic quartz, no wavy extinction	bluish-purple tuffaceous substance, brown and purple quartz	III-3 III-4
	Weakly altered diabase	Diabasic texture, silicified pyroxene, feldspar unchanged, polysynthetic twin still seen	Nonluminescent-dark purple quartz, bright green-white feldspar	III-15 III-16
	Quartz porphyry	Quartz separates sorted	Light brown quartz	III-20
Mineralized rocks, ores and quartz veins	Silicified quartz-structure rubble	Siliceous quartz lenses formed by squeeze of fractured fault structure	Dark brownish purple lenticular quartz	III-17 III-18
	Highly silicified rock	Anhedral granular quartz, fine quartz aggregates intersected by coarse ones	nonluminescent-dark purple quartz, light green sphalerite	III-5 III-6
	Highly silicified primary ore	Subhedral-anhedral siliceous quartz, medium-fine grained, without wave distinction, late-stage carbonatized replacement penetrating silicified quartz	Nonluminescent quartz with some being dark purple	III-21 III-22 III-23 III-24 III-25 III-26
	Silicified quartz vein	Quartz-vein replacement penetrating wall rocks; subhedral-anhedral quartz without wave distinction	Light purple clastic quartz in wall rocks, nonluminescent-dark purple vein quartz	III-7 III-8 III-27 III-28
	Oxidized ore	Silicified quartz reworked by post-oreforming hydrothermal and supergene solutions penetrating wall rocks	Bluish purple tuffaceous substance, brown quartz with remnant nonluminescent-dark purple quartz	III-29 III-30
	Supergene comby quartz	Thin sections made by single-grain quartz	Brown quartz	III-19

Note: Analyzed by Lu Qiuxia, the Institute of Sedimentary Geology, Chengdu Institute of Technology.

and degree of lattice order.

The experiment in this study was performed with the China-made ШхПу-3 cathodoluminescence instrument in conjunction with the Opton microscope and accessory camera. The polished thin sections are 0.03–0.04 mm thick and fixed by epoxy resin with both surfaces polished. Conditions of irradiation are as follows: beam voltage 18-20 kV, beam current 450-500 μA, electron-beam spot no less than 5 mm, ASA1600 Fuji colour film and exposure interval 13–15 min.

Table 1 indicates that silica and quartz of all host rocks are more or less luminescent but siliceous quartz in typical hydrothermal silicified quartz veins, highly silicified quartzite and primary ores shows no luminescence; whereas siliceous quartz in oxidized ores and supergene comby quartz veins irradiates brown light. It is interesting to note, however, that primary siliceous quartz is nonluminescent, and that oxidized quartz and supergene quartz show dark purple and brown light respectively. Typical photos for this case are III-22 and III-24 (nonluminescent), III-6 and III-26 (from nonluminescent to dark purple), III-28 (dark purple quartz disseminated by brown quartz), III-30 (brown quartz with remnant dark purple quartz), III-19 (brown quartz formed in supergene solutions). It is therefore clear that luminescence of oxidized supergene quartz is caused by such activators as Fe^{3+}, Ti and Mn resulting from partial dissolution of the host rocks in post-

mineralization and supergene stages. As shown in Photo III-2, the rim of secondary growth of pale purple-purple sedimentary clastic quartz irradiates brown light, revealing the luminescence of quartz related to dissolution of host rocks and also the cause of luminescence of oxidized and supergene quartz.

Correspondingly, Photo III-8 shows luminescence of silicified quartz veins penetrating clastic rocks. It is quite different from that of sedimentary clastic quartz. The former is nonluminescent while the latter shows a light purple colour. Besides, the sedimentary clastic quartz shows no corrosion. This indicates that silica causing hydrothermal silicification bears no relation with sedimentary clastic host rocks. Then is there any link between the silica and magmatic host rocks?

Lai Yong (1995) applied the cathodoluminescence technique to gold ore occurring in the faulted contact zone of migmatic gneiss and monzonitic granite, revealing that in the principal mineralization stage hydrothermal silicified quartz and clastic quartz in migmatite both show evident luminescence. He further conducted a systematic study of inclusions and proved that both silica and ore-forming solutions in hydrothermal quartz were derived from migmatic wall rocks. Obviously, in the wall rocks, tuffaceous substances in tuff, feldspar in diabase and quartz in quartz porphyry are all luminescent and moreover sponge-spicule siliceous rock has clear luminescence. It differs from nonluminescent ore-forming hydrothermal silicified quartz since the former was formed at relatively high temperatures (>573°C) and contained some colour-causing agents, while the latter had relatively low formation temperatureswithout colour-causing agent (< 300°C). Photo III-18 shows dark brownish purple light of siliceous quartz rubbles. This might result from high temperatures of over 300°C due to tectonism and might be also caused by mechanical participation of some compositions in wall rocks by way of structural fissures.

The cathodoluminescence principle (Song, 1993; Song and Yao, 1992) elucidates that besides other factors such as low temperature (<300°C), absence of colour-causing agents and high degree of lattice order, one more reason responsible for the nonluminescence of quartz might be the low degree of textural order, which brings about a trace amount of quenching impurities. The quenching impurities mainly include such elements as Fe^{2+}, Co and Ni that tend to restrain the luminescence of minerals. These elements are typically deep-derived ones. In general, quartz has a firm and enclosed texture so as to refuse impurities, but its degree of order may lower with fast cooling or crystallization to cause local disorder of inside particles and a few vacancies for a small amount of quenching impurities. This kind of impurities were really discovered by neutron activation analysis of trace elements performed in this study for vein quartz of the ore-forming stage (Liu et al., 1997). The analysis also shows that the homogenization temperature of quartz is usually below 300°C (Ni et al., 1997). This result provides evidence for nonluminescence of primary silicified quartz and meanwhile gives an indirect explanation that hydrothermal ore solutions were likely derived from the deep crust or upper mantle.

4 Composition Characteristics and Tracing Analysis of Silicon Isotopes

A Comparison of gold grades listed in Table 2 shows the following.

Rock samples showing no obvious alteration or only weak alteration or silicification (Nos. 1, 3, 5, 7, 9, 10, 14 and 17) have a gold content around or less than 30×10^{-9} (No.17 is a quartz porphyry sample). Rock samples with silicification, pyritization and arsenopyritization (Nos.2, 4, 6, 8, 11 and 15) have a gold content ranging from 0.2×10^{-6} to 2.0×10^{-6}. Vein quartz samples (Nos. 12, 23 and 16) have a very low gold content ($<0.2\times10^{-6}$). Clay (Nos.18–22) is a gold-bearing mineral thanks to its own crystallochemical features. It is thus clear that siliceous hydrothermal solutions served as fluids for carrying ore-forming minerals during mineralization. Siliceous substances in the solutions, however, were separated from the ore-forming minerals during crystallization and the ore-forming minerals then chose sulphides and clay minerals as their carriers. Among the four groups of samples mentioned above, the first represents wall rocks, the second and third siliceous hydrothermal solutions and the fourth, clay minerals, are products of siliceous hydrothermal and supergene solutions.

Table 2 Silicon isotope compositions and gold grades of host rocks, ores, quartz veins and clay minerals from the gold deposits in the study area

Ser. No.	Sample No.	Rock or mineral	δ^{30}Si ‰	Au($\times10^{-9}$)	Sampling area and horizon
1	XQG-11	Sponge-spicule siliceous rock	0.0	5.9	Roof of Dachang bed in Getang Au deposit (Dalong Formation)
2	XQG-27	Siliceous breccia (primary ore)	−0.1	8778.3	Orebody in Dachang bed of Getang Au deposit
3	XQD-20	Weakly altered basalt	0.1	18.8	Roof of Dachang bed in Qinglong Sb (Au) deposit
4	XQD-13	Silicified breccia	−0.4	120.0	Orebody of Dachang bed in Qinglong Sb (Au) deposit
5	XQL-8	Weakly altered calcareous quartz siltstone	0.0	27.6	Wall rock in T_2by of Lannigou Au deposit
6	XQL-15	Quartz-structure breccia (primary ore)	−0.2	5457.2	Orebody in T_2by of Lannigou Au deposit
7	Ms94-4	Weakly altered silty mudstone	0.3	48.6	Wall rock in T_2b of Mingshan Au deposit
8	Ms94-15	Highly altered cataclasite	−0.2	3268.0	Orebody in T_2b of Mingshan Au deposit
9	XGL-30-1	Tuff with pyrite crystal fragments	−0.2	32.1	Wall rock in P_2 of Longhuo Au deposit
10	XGL-31	Weakly altered vitroclastic tuff	−0.1	14.5	Wall rock in C_1y of Longhuo Au deposit
11	XGL4-20	Highly altered breccia (mineralized)	0.3	431.8	Orebody in C_1y of Longhuo Au deposit
12	L3-5	Quartz vein in late mineralization stage	0.5	209.2	Orebody in C_1y of Longhuo Au deposit
13	XGL4-16	Supergene comby quartz vein	0.4	56.0	Orebody in C_1y of Longhuo Au deposit
14	XGS-10	Weakly silicified diabase	0.4	32.1	Host rock in Shijia Au deposit, Indosinian
15	XGS-2	Highly altered diabase	0.4	1823.1	Primary ore in Shijia Au deposit
16	XGS-3-2	Quartz vein in late mineralization stage	0.3	22.6	Orebody of Shijia Au deposit
17	XGB-0	Quartz	0.0	5.9	Quartz porphyry vein in Bama, Guangxi
18	XQG-24-1	Kaolinite	−0.2	1054 *	Oxidized ore of Dachang bed in Getang Au deposit
19	XGL-4-10-1	Illite	0.4	1094.2	Oxidized ore in C_1y of Longhuo Au deposit
20	XGL-1-3	Illite	0.2	8013.2	Primary ore in C_1y of Longhuo Au deposit
21	XQL-23-2	Illite	0.6	21.5 ($\times10^{-6}$)	Oxidized ore in T_2by of Lannigou Au deposit
22	XQL-20-1	Illite	0.2	2292.9	Primary ore in T_2b_y of Lannigou Au deposit

Notes: Analyzed by the Institute of Mineral Deposits, MGMR (analytic precision>0.1 ‰); * after Cheng Feng and Yang Keyou (1992); Au contents obtained by neutron activation analysis, performed by the Neutron Activation Lab of the Third Department, the Chengdu Institute of Technology.

The results in Table 2 are illustrated in Fig. 3, which shows the following.

(1) Distinct difference is seen in δ^{30}Si between the host rocks (including basalt) and the mineralized rocks or primary siliceous ore in Getang, Qinglong, Lannigou and Mingshan. The former (Nos.1, 3, 5 and 7) range from 0.0 ‰ to 0.3 ‰, while the latter (Nos.2, 4, 6 and 8) from −0.1 ‰ to −0.4 ‰. Cathodoluminescence analysis shows that clastic quartz in the host rocks, such as siliceous and clastic sedimentary rocks, is luminescent (Photos III-2, 12 and 14), but siliceous quartz in neighbouring primary ores is nonluminescent (Photos III-8, 24 and 26). Thus we can see that silica in the host rocks is not related to that formed after mineralization and superposition.

(2) Great difference of the δ^{30}Si values can be seen between the weakly altered host rocks (Nos. 9 and 10) in the Upper Permian and Lower Carboniferous and mineralized rocks, ores and hydrothermal quartz veins (Nos. 11, 12 and 13) in the Lower Carboniferous in the Longhuo gold deposit. The former ranges from −0.1 ‰ to −0.2 ‰, while the latter from 0.3 ‰ to 0.5 ‰. Cathodoluminescence analysis shows that clastic quartz in the host tuffaceous rocks is quite diversified in colour (Photos III-3 and 4) with rather low maturity, implying different but less distant sources of the clasts. However, siliceous quartz in neighbouring primary ores is nonluminescent (Photos III-22 and 24). This indicates that siliceous substances in the host rocks are not related to those formed after mineralization and superposition.

(3) In the Shijia deposit, the δ^{30}Si values of the major host rock (No.14), Indosinian diabase veins, are very close to those of the primary ore and ore-forming quartz veins (Nos.15 and 16), ranging from 0.3 ‰ to 0.4 ‰. Does this mean that ore-forming siliceous solutions came from the Indosinian diabase?

Identification of thin sections of weakly altered diabase (Photo III-15) reveals that this weak alteration is manifested by silicification of pyroxene crystals and high gold content, being several times as large as the background (Table 2). Obviously, this rock has been subjected to weak alteration from ore-forming siliceous fluids, evidenced by remaining basic plagioclase. One

can easily explain from the view of mineral crystallochemistry that pyroxene has stronger ability (aptness) than plagioclase to accept siliceous substences. It is thus understood that the consistency of their $\delta^{30}Si$ values does not mean that diabase veins provide silica or other ore-forming substances for mineralization. Moreover, $\delta^{30}Si$ of weakly altered diabase veins (0.4 ‰) is notably higher than that of general mafic rocks (<0.0 ‰) (Ding et al., 1994), implying that such rocks were once subjected to fluid reworking after their formation. This agrees with the result of thin section identification.

Very weak mineralization but no weak silicification of the Middle Triassic host rocks was observed in the Lannigou and Mingshan deposits. This is because that siltstone and mudstone do not contain basic minerals, and are thus more resistant to silicification and easier to accept mineralized diffusion halos. As a result, siliceous diffusion halos are less extensive than mineralized ones. This feature can also be seen in other ore districts. This is good for studying the relationships between host rocks and orebodies in an ore district by means of silicon isotopes.

Douthitt's study revealed (1982) that $\delta^{30}Si$ of dissolved silica is not related to silicon content in the solution and is not related to solution temperature either as the temperature ranges from 75°C to 275°C. This suggests that $\delta^{30}Si$ of dissolved siliceous in a hydrothermal system is likely controlled by the source of the silica. The above discussion proves from different angles that the distinction of $\delta^{30}Si$ between host rocks and ore-forming siliceous hydrothermal solutions indicates different sources of siliceous substances.

(4) Illite and kaolinite have very different $\delta^{30}Si$ values, the former ranging from 0.2 ‰ to 0.6 ‰ while the latter being −0.2 ‰. Besides, the $\delta^{30}Si$ values of illite are different between oxidized and primary ores with the former (0.4 ‰–0.6 ‰) being higher than the latter (0.2 ‰) even in the same horizon of the same ore district or in different horizons of different ore districts. This not only implies that silicon isotopic compositions experience further fractionation as primary ores transform into oxidized ones, but more importantly proves that silicification of the gold ore in the study area should belong to the same ore-forming siliceous fluid, which is in agreement with the understanding that the period from the late Yanshanian to the early Himalayan is the metallogenic epoch in this area.

Furthermore, distinction of silicon isotopic compositions between kaolinite and illite might also be related to fractionation of silicon isotopes between these two minerals due to their different crystalline textures.

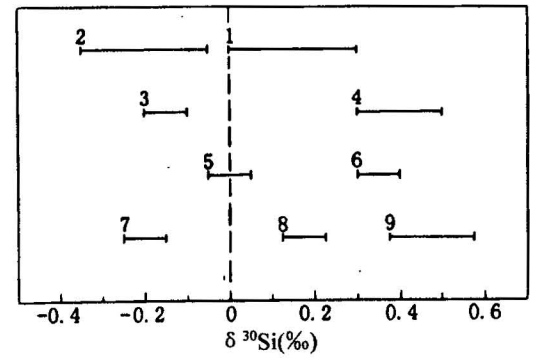

Fig. 3. Diagram of distribution of silicon isotope compositions of host rocks, mineralized rocks, ores, quartz veins and clay minerals in the gold deposits of the study area.

1. Host rocks of the Getang, Qinglong, Lannigou and Mingshan gold deposits (Dachang bed and T_2); 2. mineralized rocks, ores and quartz veins of the Getang, Qinglong, Lannigou and Mingshan gold deposits; 3. host rocks of the Longhuo gold deposit (P_2 and C_1); 4. mineralized rocks and quartz veins of the Longhuo gold deposit; 5. quartz in quartz porphyry; 6. weakly altered diabase (Indosinian), ores and quartz veins of the Shijia gold deposit; 7. kaolinite in oxidized ore; 8. illite in primary ore; 9. illite in oxidized ore.

The following understanding can be obtained from the evolution curve shown in Fig. 4.

(1) Disagreement exists between strata divided by the "Dachang bed" with respect to silicon isotope compositions of siliceous fluids: the newer strata correspond to negative and slightly varied values, but the older ones to positive high values; and the host rocks show fairly flat curves.

(2) Shape of the curves shows that ore-forming siliceous fluids have no effect on the host rocks, while the effect of the host rocks on the ore-forming siliceous fluids lies only in the rather low $\delta^{30}Si$ values of siliceous fluids in the "Dachang bed" as they change from negative to positive or from positive to negative. This is probably related to the participation of low $\delta^{30}Si$ values of the Upper Permian tuffaceous rocks owing to intense interlayer gliding (detachment) of the "Dachang bed".

(3) $\delta^{30}Si$ of clay minerals varies moderately from

low to high as the mineral changes from kaolinite→illite in primary ore→illite in oxidized ore.

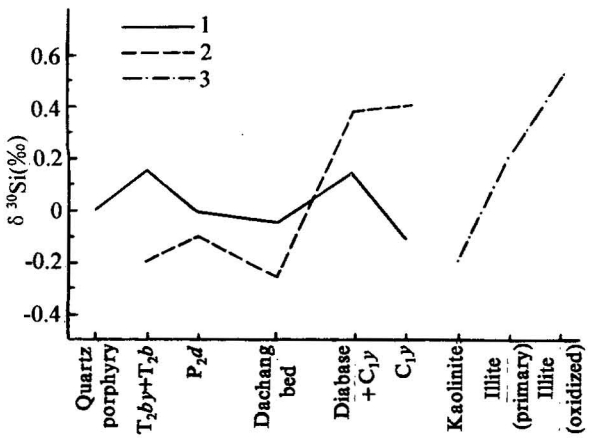

Fig. 4. A diagram showing silicon isotope compositions of host rocks and ore-forming siliceous fluids of the gold deposit in the study area.

1. Curve of host rock; 2.curve of ore-forming siliceous fluid; 3.curve of clay mineral.

5 Dynamic Mechanism of Silicon Isotope Fractionation and Possibility of Deep Metallogenesis

From Fig.4 one can see that $\delta^{30}Si$ of siliceous fluids changes from negative (−0.4 ‰ to −0.3 ‰) to positive (0.3 ‰ to 0.5 ‰) as the strata change from younger one (T_2) through P_2 and the "Dachang bed" to older one (C_1y) and Indosinian diabase. We consider that this change mainly depends on dynamic fractionation of silicon isotopes during the migration of fluids.

A great deal of research has proved that the $\delta^{30}Si$ values of silica first precipitated in the extrusion of siliceous fluids are generally negative. The following examples can be given for this case. In Tengchong, Yunnan Province, $\delta^{30}Si$ values of hot spring quartz veins, sinter and spring water correspond to −0.6 ‰, −0.1 ‰ and 0.3 ‰, respectively (Ding et al., 1996); in the Gongchangling iron deposit, $\delta^{30}Si$ of Archaean and Proterozoic magnetite quartzite ranges from −0.9 ‰ to −2.2 ‰ (Ding et al., 1994), which is very close to that of modern sea-floor exhalation-sedimentary silica (−0.4 ‰ to −3.1 ‰) (Hou et al., 1996); Hutchinson (1973, 1984) held that most of the Precambrian banded Si-Fe formations were probably deposited from siliceous hydrothermal fluids during sea-floor convection; in the Honghuagou gold deposit in Chifeng, Inner Mongolia, hosted in Archaean compound gneiss, the $\delta^{30}Si$ values of hydrothermal quartz veins are from −0.1 ‰ to −0.2 ‰ (Ding et al., 1996). As mentioned above, the metallogenic epoch of Carlin-type gold ore in this area is the period from the late Yanshanian to early Himalayan, during which deep ore-bearing siliceous fluids migrated upwards along deep-seated faults rapidly driven by thermodynamics due to tectonism and diapiric magmatism and during this process the fluids themselves had no silicon isotope fractionation; relative intense dynamic fractionation occurred as the fluids moved into secondary ore-hosting structures where they could stay for a longer period than in deep layers due to more favourable conditions and the silica could be crystallized more slowly, so that $\delta^{30}Si$ values of the primary silica in shallow layers are lower than those of older layers. However, a longer stay of ore-forming fluids in secondary host structures would naturally lead to contamination and metasomatism, weakly or strongly, with the wall rocks. This shows that relatively large depth and enclosed environment are favourable conditions for mineralization and in turn present good prospects in searching for this type of gold ore.

Li et al. (1994) bore out the dynamic fractionation of silicon isotopes and measured the fraction coefficients α_{Si}, ranging from 0.9990 to 0.9996, indicating that $\delta^{30}Si$ of precipitated silica resulting from the dynamic fractionation varies within a range of 1.0 ‰ compared with that of dissolved silica. The variation can be described by Reyleigh's Equation (Fig. 5). Now that dynamic fractionation of silicon isotopes occurred in ore-bearing siliceous fluids, the $\delta^{30}Si$ values of siliceous precipitates in primary silica of different horizons can be used to semiquantitatively simulate the precipitation and crystallization processes of silica in the fluids. It is estimated based on Fig. 4 that $\delta^{30}Si$ of primary silica in relatively new host strata varies from −0.4 ‰ to −0.1 ‰ and the maximum proportion of silica precipitates is about 43%–57%; whereas $\delta^{30}Si$ for relatively old strata is 0.3 ‰–0.5 ‰ and the corresponding proportion is 72%–79%. It is believed that larger quantity of precipitated SiO_2 may lead to larger quantity of ore-forming minerals. It is therefore expected that large or superlarge gold ore deposits will

more likely occur in depths.

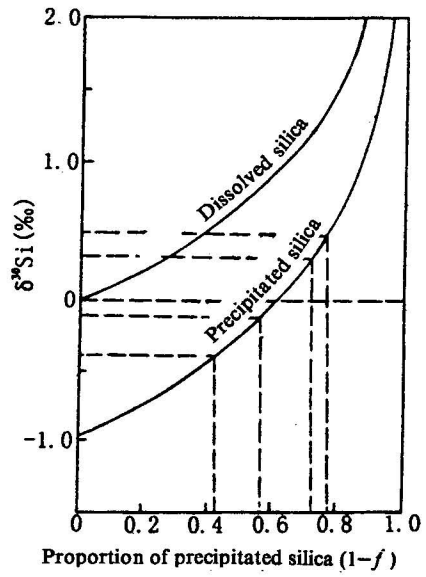

Fig. 5. Curves of silicon isotope dynamic fractionation in the process of precipitation of silica in fluids (after Li et al., 1994). α_{Si}=0.9990–0.9996; $\delta^{30}Si_{\Sigma Si}$=0.0 ‰.

Moreover, δ^{30}Si of quartz in quartz porphyry (0.0 ‰) is the same as that of S-type granite porphyry in Dasi, Guangxi (Ding et al., 1994), probably representing the practical silicon isotope value, which is between the δ^{30}Si values of the two ore-forming siliceous fluids in the study area. The dynamic fractionation mechanism between dissolved and precipitated silica tells us that if the ore-bearing siliceous solution is from quartz porphyry, δ^{30}Si of the first precipitated silica will be positive, if not very large, and the ensuing precipitates have even larger δ^{30}Si values. This fact is contradictory to the case with the gold deposits in this area and at the same time the quartz in quartz porphyry shows brown light under cathodoluminescence. Subsequently, quartz porphyry cannot provide silica for ore formation. Nevertheless, quartz porphyry was formed in the Yanshanian (Yang et al., 1994) and has almost the same petrogenic and metallogenic epoch, hence it gives direct evidence for the thermodynamic condition given by magmatism in the metallogenic process.

6 Conclusions

(1) Neither silicon isotope fractionation nor compositional replacement with the wall rocks could occur for Si-enriched ore-forming fluids when migrating rapidly upwards along deep-seated giant faults, unless the fluids injected into secondary host structures of different strata, and the fractionation and replacement were more intense in deeper layers. Therefore, δ^{30}Si of primary silica in newer strata is lower than that of older ones. Besides, contamination and replacement would inevitably occur between fluids and wall rocks in host structures at different depths. This is favourable for ore formation, especially in deep layers.

(2) Silica was generally precipitated in superimposed silicified layers. Analysis of gold grade shows that superimposed silicified layers are the major superimposed mineralized positions. This clearly explains that siliceous fluids serve as ore-bearing solutions.

(3) Silicon isotope study coupled with siliceous cathodoluminescence analysis reveals that wall rocks (including magmas) and mineralized rocks have different siliceous sources, so do ores and ore-forming quartz veins. As a result, neither wall rocks nor magmatic rocks can supply ore-forming minerals. At least they are not the major source of mineralized substances, which were derived mainly from deep layers.

(4) Mechanism of dynamic fractionation of silicon isotopes along with cathodoluminescence analysis as well as metallogenic age analysis shows that silicification results from the same ore-bearing siliceous fluid even for different horizons of different deposits. If additional analyses are performed (Ni et al., 1997; Liu, Ni and Su, 1996; Liu, Jin and Ni, 1996; Liu et al., 1997) we may conclude that silica and ore-forming minerals might come directly from the upper mantle.

(5) Based on measurements of δ^{30}Si values of primary silica in different horizons and semiquantitative simulation of precipitation and crystallization of silicon in ore-forming siliceous fluids one can understand that precipitated SiO_2 in deep-seated favourable host structures is far more than that in shallow positions, indicating that a deep enclosed environment is very favourable for gold ore and that, more importantly, contamination and metasomatism in these deep structures might provide significant geochemical background for large and superlarge gold deposits. Therefore, there are fairly good prospects in searching for Carlin-type gold ore deposits there.

(6) In the gold deposits in the Yunnan-Guizhou-Guangxi triangle area, silicified diffusion halos spread

generally in narrower areas than mineralized ones except for basic host rocks, so silicon isotope geochemistry in combination with siliceous cathodoluminescence can be effectively applied to studying and discussing sources of the ore minerals of Carlin-type gold deposit.

Acknowledgements

This study was jointly supported by the key research project for gold prospecting during the Eighth Five-Year Plan period (KY85-12-04-02) and the Open Lab of Deposit Geochemistry of Chinese Academy of Sciences. Thanks are also due to Profs. Yang Keyou, Li Chaoyang, Hu Ruizhong, Gao Zhenmin and Ding Tiping for their guidance, support and assistance in this research and to Dr. Zhang Xingchun and Associate Prof. Su Wenchao for their help in field work.

Chinese manuscript received Aug. 1997
accepted March 1998
edited by Zhang Yuxu
translated by Liu Xinzhu

References

Ding Tiping, Jiang Shaoyong, Wan Defang, Li Yanhe et al., 1996. Silicon Isotope Geochemistry. Beijing: Geological Publishing House, 23–58 (in Chinese).

Douthitt, C.B., 1982. The geochemistry of the stable isotopes of silicon. *Geochim. Cosmochim. Acta*, 46(8): 1449–1458.

Hou Zengqian Wu Shiying and Urabe, T., 1996. The isotopic compositions of silicon and oxygen of siliceous rocks in the kuroku-type deposits, Gacun, Sichuan, as compared with those of siliceous chimney on modern seafloor. *Geological Review*, 42(6): 531–540 (in Chinese with English abstract).

Hu Ruizhong, Su Wenchao, Li Zeqin et al., 1995. A possible evolution path of the ore-forming hydrothermal solution for micro-disseminated gold deposits in the Yunnan-Guizhou-Guangxi "Triangle Area"— Geochronological evidence. *Acta Mineralogica Sinica*, 15(2): 144-149 (in Chinese with English abstract).

Hutchinson, R.W., 1973. Volcanogenic sulfide, deposits and their metallogenic significance. *Econ. Geol.*, 68(6): 1223–1246.

Hutchinson, R.W., 1984. Some broad characteristics of greenstone belt gold lodes. *Gold*, 82(2): 339–371.

Lai Yong, 1995. Metallogenic conditions and process of the Wendeng gold deposit, Shandong. *Mineral Deposits*, 14(3): 281–289 (in Chinese with English abstract).

Li Yanhe, Ding Tiping and Wan Defang, 1994. Dynamic fraction of silicon isotopes — experimental studies and geological applications. *Mineral Deposits*, 13(3): 282–287 (in Chinese with English abstract).

Liu Xianfan, Ni Shijun and Su Wenchao, 1996. Isotope geochemistry of the micro-disseminated gold deposits in the Yunnan-Guizhou-Guangxi area and its implications for deep-source fluids. *Minerals and Rocks*, 16(4): 106–111 (in Chinese with English Abstract).

Liu Xianfan, Jin Jingfu and Ni Shijun, 1996. The deep origin of ore-metals in micro-disseminated gold deposits, Yunnan-Guizhou-Guangxi region–REE evidence. *Journal of Chengdu Institute of Technology*, 23(4): 25–30 (in Chinese with English abstract).

Liu Xianfan, Liu Jiajun, Zhu Laimin and Lu Qiuxia, 1997. Lead isotopic compositions of the micro-disseminated gold deposits, Yunnan-Guizhou-Guangxi region and their applications. *Bulletin of Mineralogy, Petrology and Geochemistry*, 16(3): 178–182 (in Chinese with English abstract).

Liu Xianfan, Ni Shijun and Jin Jingfu, 1997. Source of ore-metals in micro-disseminated gold deposits in the Yunnan-Guizhou-Guangxi region — Trace element evidence. *Geotectonica et Metellogenica*, 21(3): 205–212 (in Chinese with English abstract).

Ni Shijun, Liu Xianfan, Jinjingfu and Lu Qiuxia, 1997. Geochemistry of the Ore-forming Fluid in Micro-Disseminated Gold Deposits, the Yunnan-Guizhou-Guangxi "Triangle Area". Chengdu: Chengdu Science and Technology University Press, 36–96 (in Chinese).

Song Zhimin and Yao Yong, 1992. Applications of cathodoluminescence in the study of ore deposits — with Jinding Pb-Zn deposit, Yunnan, as an example. *Modern Geology*, 6(2): 139–149 (in Chinese with English abstract).

Song Zhimin, 1993. Geological Basis of Cathodoluminescence. Wuhan: China University of Geosciences Press, 45–49 (in Chinese).

Wang Yangeng, Wang Liting and Zhang Mingfa, 1995. Structure of the shallow crust and the distribution model of gold deposits in the Nanpanjiang region. *Guizhou Geology*, 12(2): 79–100 (in Chinese with English abstract).

Xia Bangdong, Liu Honglei and Wu Yungao, 1992. The Yunnan-Guizhou-Guangxi rift. *Experimental Petroleum Geology*, 14(1): 20–30 (in Chinese with English abstract).

Yang Keyou, Chen Feng, Su Wenchao et al., 1994. Carlin-type gold deposits in the Yunnan-Guizhou-Guangxi area — Geological-geochemical characters and prospecting. A Comparative Study of Chinese and Canadian Gold Deposits – CIDA II-17 paper Collection, Beijing: Seismological Press, 17–30 (in Chinese).

About the first author

Liu Xianfan Born in June 1957; obtained his B.Sc., M.Sc and Ph.D at the Chengdu College of Geology in 1982, 1990 and 1996, respectively, and then has been conducting postdoctoral research as Associate Professor in the Institute of Geochemistry, Chinese Academy of Sciences. Dr. Liu has long been engaged in teaching and research work of mineralogy and geochemistry of mineral deposits.